ISTITUTO NAZIONALE DI FISICA NUCLEARE

Sezione di Genova

**INFN-23-24/GE**
**1 Giugno 2023**

# Assessment of hadronic reactions in GEANT4 and FLUKA for the POKER experiment

Pietro Bisio[1,2], Mariangela Bondì[3], Andrea Celentano[1], Anna Marini[1], Luca Marsicano[1]

[1)] *INFN, Sezione di Genova, 16147 Italy*

[2)] *Università degli Studi di Genova, Genova, 16100 Italy*

[3)] *INFN, Sezione di Catania, 95125 Italy*

**Abstract**

The goal of the POKER ERC project is to establish and demonstrate a new approach to the search for light-dark matter, based on a missing energy measurement with a positron-beam, active thick-target setup. In the experiment, a high-energy $e^+$ beam impinges on a high-performance hermetic calorimeter, that measures the deposited energy event by event. Light dark matter particles could be produced by the annihilation of the positron with atomic electrons, and would then escape from the detector without further interactions.

One of the most critical background reactions for the measurement involve one or more high-energy hadrons produced by the developing electromagnetic shower and escaping from the calorimeter, thus resulting in a sizeable missing energy. A Monte Carlo estimate of this background yield is required in order to properly design the experimental apparatus. In order to validate the simulation results, we compared the predictions from the FLUKA and GEANT4 Monte Carlo programs with available data for a few hadronic reactions involving long-lived neutral hadrons or particles emitted at backward angles. Our results show that, in general, the agreement between the Monte Carlo predictions and the real data is good, with FLUKA results closer to the experimental measurements, in particular concerning the shape of the cross section.

PACS:13.40.-f,13.85.Ni,13.85.Lg,02.70.Uu

*Published by*
*Laboratori Nazionali di Frascati*

## 1 Introduction

### *1.1 The POKER experiment*

The several hints suggesting the existence of dark matter (DM) are a "smoking gun" evidence of physics beyond the Standard Model (SM). However, all experimental evidences are based on gravitational effects, and so far we know nothing about the DM particle content: uncovering this puzzle is a top priority in fundamental physics. Until today, the theoretical and experimental efforts have mainly focused on the WIMPs (Weakly Interacting Massive Particles) scenario [1] - however, null results in direct detection experiments of galactic halo DM and in high-energy accelerator searches at the LHC call for an alternative explanation to the current paradigm [2]. The light dark matter (LDM) hypothesis conjectures the existence of a new class of lighter elementary particles, not charged under the SM interactions. The simplest model predicts LDM particles with masses below 1 GeV/$c^2$, charged under a new force in Nature and interacting with the SM particles via the exchange of a light spin-1 boson, usually referred to as "dark photon" (A') [3]. This picture foresees the existence of a new "Dark Sector" , with its own particles and interactions, and is compatible with the well-motivated hypothesis of DM thermal origin [4].

The scope of the POKER experiment is to establish and demonstrate a new approach to search for light dark matter at accelerators, based on a missing energy measurement with a positron-beam, active thick-target setup, to exploit resonant A' production through positrons annihilation on atomic electrons. This resonant mechanism corresponds to a large yield of signal events, and is characterized by a unique kinematic signature: a well-defined missing energy value, that depends solely on the A' mass [5]. The goal of POKER is to validate experimentally the new technique. To do so, POKER will prepare and run a short pilot experiment exploiting the high-energy ($\sim$ 100 GeV) $e^+$ beam available at the CERN H4 beamline, with a foreseen accumulated statistics of approximately $10^{11}$ positrons-on-target ($E^+OT$) within a few weeks running time. Since this will be the first time that a fixed-target missing energy measurement with a positron beam will be realized, the main focus will be the characterization of the different background sources and the development of analysis strategies to mitigate them. To focus on the scientific validation of the new approach and to optimize resources, the POKER strategy is to minimize the risks connected to the technologies required to build the detector, in order to be able to complete the pilot run within the five-years time scale of the ERC project. In particular, POKER plans to re-use the already-existing components developed by the NA64 collaboration for their $e^-$ beam missing-energy program at the same facility [6]. These include the hadronic calorimeter installed downstream of the active target (HCAL), the upstream synchrotron-radiation-based beam tagging system (SRD), the high-efficiency plastic scintillator counter between the ECAL and the HCAL (VETO), and the trigger and data acquisition system. For the same reasons, the new POKER high-resolution active target (ECAL) will be developed exploiting well-known and robust technologies: the leading option is to use $PbWO_4$ scintillating crystals with SiPM readout. If successful, POKER will permit the establishment of the scientific basis for the first high-statistics LDM search experiment at a positron-beam facility.

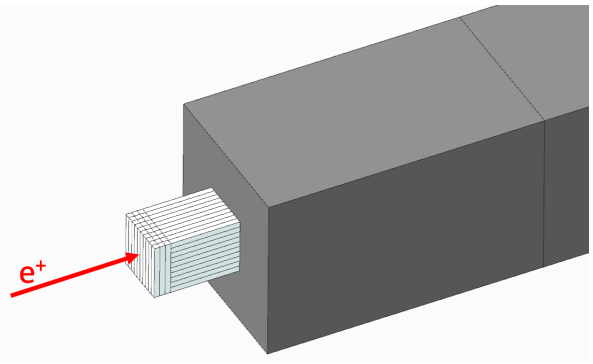


Figure 1: Schematic layout of the POKER detector, showing the $PbWO_4$ calorimeter (white) and a portion of the hadron detection system (gray). The upstream SRD beam monitor and the VETO counter between the ECAL and the HCAL are not shown.

### *1.2 Signal and background*

**Signal properties** The cross-section for LDM production through positron annihilation on atomic electrons is characterized by a resonant shape:

$$\sigma = \frac{4\pi\alpha_{EM}\alpha_D\varepsilon^2}{\sqrt{s}} \frac{q(s-4/3q^2)}{(s-m_{A'}^2)^2+\Gamma_{A'}^2 m_{A'}^2} \quad , \tag{1}$$

where $s$ is the $e^+\ e^-$ system invariant mass squared, $q$ is the $\chi-\overline{\chi}$ momentum in the CM frame, and $\Gamma_{A'}$ is the $A'$ width. This cross-section exhibits a maximum at $s = m_{A'}^2$, i.e. at positron energy $E_R \simeq m_{A'}^2/(2m_e)$. From energy conservation, it follows that $E_{e^+} \simeq E_{A'} = E_\chi + E_{\overline{\chi}}$. As a consequence, the distribution of the energy sum of the final state $\chi-\overline{\chi}$ pair and, by extension, of the $s-$channel dark photon also shows a maximum at this energy value. This introduces a very peculiar kinematic feature of the signal events, that result in a peak in the missing energy ($E_{miss}$) distribution, whose position depends solely on the $A'$ mass through the kinematic relation

$$m_{A'} = \sqrt{2m_e E_{miss}}\ ; \tag{2}$$

the width of the peak is determined by the convolution between the resonant shape and the active thick-target energy resolution.

**Background sources** The most critical background reactions for a missing energy measurement involve one or more high-energy neutral hadrons produced by the developing electromagnetic shower and escaping from the calorimeter without being detected in the downstream HCAL, thus mimicking the signal missing energy signature. Although the total HCAL length corresponds to approximately 30 nuclear interaction lengths, resulting in a hadron punch-through probability of about $10^{-13}$, still it is of uppermost importance for the experiment to strictly control this background source, in order to compensate for effects such as inhomogeneities in the HCAL geometry, or variations in the detection thresholds, that would lower the detection efficiency. This is true both for the intensity of these processes and for the kinematic distribution of the produced hadrons.

Following the collision of a high-energy GeV positron on the ECAL, the production of high-energy hadrons in the detector volume, at first order, results from the following reactions:

- photoproduction reactions involving a secondary photon of the electromagnetic shower interacting with an atomic nucleus, $\gamma N \to X$.

- Electro-production reactions involving a positron or an electron of the electromagnetic shower interacting with an atomic nucleus, $eN \to e'X$.

In the following, we denote with $\vec{x}$ a complete set of kinematic variables to describe the hadronic component of the final state being considered. The total yield of events, taking into account the development of the electromagnetic shower, reads:

$$\frac{dN}{d\vec{x}} \propto \int dE\, T(E) \frac{d\sigma}{d\vec{x}}(E) \quad , \tag{3}$$

where $T(E)$ is the track-length distribution of photons/electrons and positrons in the thick target [7]. It should be noted that, since in the electro-production case the final state electron/positron is always absorbed in the ECAL, the total contribution to the yield of hadronic events is obtained by integrating the corresponding cross-section over all possible values of the final state lepton energy $E_{e'}$ and angle $\theta_{e'}$,

$$\frac{d\sigma}{d\vec{x}} = \int dE_{e'} d\cos(\theta_{e'}) \frac{d\sigma}{dE_{e'} d\cos(\theta_{e'}) d\vec{x}} \quad . \tag{4}$$

In the one-photon-exchange approximation [8], due to the kinematic shape of the electro-scattering cross-section, the previous integral gets the largest contribution for $\theta'_e \simeq 0$, i.e. most of the electro-production events are characterized by a very small value of the electron scattering angle. This is the so-called "quasi-real photoproduction" case, in which $Q^2 \simeq 0$, and in which the polarization matrix of the virtual photon resembles that of a real photon, with the longitudinal terms suppressed by a factor $Q^2$ with respect to the transverse ones. In this regime, the differential electro-production cross-section can be factorized as:

$$\frac{d\sigma}{dE_{e'} d\cos(\theta_{e'}) d\vec{x}} \simeq \frac{d\sigma^{\gamma}}{d\vec{x}}(\nu) \cdot \frac{d\Gamma}{dE_{e'} d\cos(\theta_{e'})} \quad , \tag{5}$$

where $\frac{d\sigma^{\gamma}}{d\vec{x}}(\nu)$ is the real photoproduction cross section for impinging photon energy $\nu \equiv E_0 - E_{e'}$ and $\frac{d\Gamma}{dE_{e'} d\cos(\theta_{e'})}$ is the virtual photon flux.

Finally, at the multi-GeV energy scale relevant for POKER, at first order the hadronic interaction of a real photon with a nucleus can be reconducted to the interaction with the constituent nucleons [9, 10]:

- For photon energies up to few GeV, but still large enough so that the photon wavelength is smaller than the intra-nuclei distances, $\sigma_{\gamma}^{N} \propto \sigma_{\gamma}^{p} \cdot Z + \sigma_{\gamma}^{n} \cdot (A - Z)$, where $A$ and $Z$ are, respectively, the mass number and the charge number of the target nucleus.

- At larger energies, where the photon-nucleus interactions are mediated by the exchange of light vector mesons according to the so-called "vector meson dominance" (VMD) model, $\sigma_{\gamma}^{N} \propto \sigma_{\gamma}^{p,n} \cdot A^{2/3}$.

In conclusion, the description of the production of high-energy hadrons due to the interaction of the high-energy GeV positrons with the POKER active thick target requires as basic ingredient the knownledge of the photon-nucleon interaction cross section for the different processes being considered. This work will thus focus on the assessment of the implementation of these cross sections in the GEANT4 and FLUKA simulation frameworks, comparing the Monte Carlo predictions with the available data. Specifically, we considered the following two benchmark reactions: the inclusive production of Lambda and anti-Lambda baryons on the proton, and the exclusive charge-exchange production of a $\pi^+$, emitted at backward angle.

## 2 Methodology

In order to validate the implementation of photoproduction reactions in the GEANT4 and FLUKA codes, we have defined a simple test-case setup, with a photon beam impinging on a $l = 1$ mm long $l\mathrm{H}_2$ target ($\rho = 0.0708$ g/cm$^3$). We then scored the four-momentum of each particle emerging from the target. In FLUKA, this was done by means of a custom `mgdraw` user routine, producing a ROOT `TTree` with one row for each produced particle due to the interaction of the impinging photon with the target. In GEANT4, this was done through the use of a special sensitive detector placed all around the target, scoring the four-momentum of each particle passing through it.

### *2.1 Experimental data*

The results of simulations were validated by comparison with available data sets for photo-nuclear reactions on hydrogen target at multi-GeV photon energy. For the inclusive photoproduction of $\Lambda$ and $\overline{\Lambda}$, we considered the measurements performed by the SLAC Hybrid Facility Photon Collaboration [11, 12], who employed a 20 GeV monochromatic beam impinging on a 1-m diameter hydrogen bubble chamber installed within a 2.6 T magnetic field. Also, we considered the results from the Bonn-CERN-Ecole Polytechnique- Glasgow-Lancaster-Manchester-Orsay-Paris VI-Paris-Rutherfordl-Sheffield collaboration, who used a tagged photon beam in the range 25-75 GeV and the Omega spectrometer at CERN SPS, in the framework of the WA4 experiment [13]. For the exclusive $\pi^+$ production, instead, we considered the measurements from SLAC experiments, employing a Bremmstrahlung photon beam with energy in the range 5-15.5 GeV, and measuring the emitted $\pi^+$ with a single-arm spectrometer [14, 15].

### *2.2 Monte Carlo simulations details*

#### *2.2.1 Biasing*

A simple biasing scheme was introduced in the simulations in order to enhance the photon hadronic interactions in the target, by artificially multiplying the total $\gamma - p$ interactions cross section by a factor $B = 10^5$. The choice of this value is justified by the fact that the order magnitude of the total photon-nucleon cross-section $\sigma^{TOT}_{\gamma-p}$ is approximately 100 $\mu$barn, resulting to a mean free path $\lambda_\gamma = \frac{1}{n\sigma^{TOT}_{\gamma-p}} \simeq 2 \cdot 10^5$ cm. The event-by-event probability that an impinging photon interacts hadronically with the target is thus $P = l/\lambda \ll 1$. By multiplying the total cross section by the

aforementioned factor, the biased mean free path in the simulations is $\lambda' = \lambda/B \simeq 2$ cm, and the corresponding interaction probability in the target is $P' = P \cdot B = 5\%$. This value permits to obtain significant statistics of photo-nuclear hadronic events in a reasonable computation time, while still allowing to de-bias the final result by simply scaling the number of events obtained in the simulation by a factor $1/B$.

### *2.2.2 Photo-nuclear reactions implementation*

**FLUKA** FLUKA implements photo-nuclear reactions at high energies ($E_\gamma > 720$ MeV) through the VMD model. The total photo-nuclear cross-section is expressed as $\sigma_\gamma^N \propto \sigma_\gamma^p \cdot Z + \sigma_\gamma^n$, with $\sigma_\gamma^p$ and $\sigma_\gamma^n$ obtained from tabulate data. A "shadowing effect" is also introduced, as well as a correction factor to account for the asymptotic increase of the cross-section at very high energies. The production and the further interactions of the final state hadrons are described via the FLUKA hadron-nucleon inelastic collisions model [16], based on the Dual Parton Model [17] for the energy range of interest of this work.
We performed our simulations using FLUKA version `2020.0.3`, respin April 9th 2020. In order to activate photo-nuclear reactions the `PHOTONUC` card was used setting $WHAT(1) = 1$.

**GEANT4** GEANT4 implements photo-nuclear reactions at high energies using a Regge-Pomeron model. The total cross-section as a function of the impinging photon energy is parameterized as the sum of two terms, describing the Pomeron contribution and that of higher Regge trajectories, respectively [18]. The production of final state particles is described by means of a quark-gluon string model and a diffractive Ansatz for string excitation [19]. At lower energies, instead, photonuclear interactions are implemented via the Bertini cascade model [20]. This is based on a "catalog" of photon-hadron and hadron-hadron reaction tables, as well as some simple parametrizations of photon- and pion- dissociation of di-nucleons.
We performed our simulations using the GEMC interface [21] to GEANT4 version `4.10.07.p02`. In order to activate photo-nuclear reactions we used a custom physics list, with an instance of the `G4EmExtraPhysics` class, that in turns instantiates `G4BertiniElectroNuclearBuilder` object. High-energy photo-nuclear reactions are handled through the `G4TheoFSGenerator` model, while low-energy photo-nuclear reactions are handled through the `G4CascadeInterface` interface to the Bertini cascade. By default, the transition between the two regimes happens approximately at 3 GeV.

## 3 Results

We made a comparison between the available data and the results obtained from the Monte Carlo simulation frameworks for the photon-induced hadronic reactions on a proton target reported in Tab. 1.

| Case # | Reaction | Photon beam energy | Observable | Reference |
|---|---|---|---|---|
| **1** | $\gamma p \to \Lambda X$ | 20 GeV | $\sigma_{TOT}$<br>$F(x)$ | [11]<br>[12] |
| | $\gamma p \to \overline{\Lambda} X$ | | $\sigma_{TOT}$<br>$F(x)$ | [11]<br>[12] |
| | $\gamma p \to \Lambda X$ | 25-75 GeV | $\frac{d\sigma}{dx}$ | [13] |
| | $\gamma p \to \overline{\Lambda} X$ | | | |
| **2** | $\gamma p \to \pi^+ n$ | 5-15.5 GeV | $\frac{d\sigma}{du}$ | [14] |
| | | 5 GeV | $\frac{d\sigma}{dt}$ | [15] |

Table 1: Summary of the different photoproduction reactions considered in this work.

### *3.1 Case-1: $\Lambda$ and $\overline{\Lambda}$ inclusive production*

The first reaction considered in this study is the inclusive production of $\Lambda$ and $\overline{\Lambda}$ hyperons on the proton. Due to the large mean life of these hyperons ($c\tau \simeq 7.8$ cm), the inclusive production can be actually measured in POKER, by searching for events in which the $\Lambda/\overline{\Lambda}$ exits from the active target carrying a significant fraction of the primary beam energy, passes through the VETO without interacting, and then decays (or interacts hadronically) in the HCAL, depositing its energy in this detector. These channels thus represent an important benchmark channel for Monte Carlo simulations.

In both the datasets here considered, $\Lambda$ and $\overline{\Lambda}$ were identified through their $p\pi^-$ / $\overline{p}\pi^+$ decay (branching fraction $\simeq 64.2\%$), measuring the momentum of final state particles and then reconstructing the corresponding invariant mass. It should be noted that in both experiments it was not possible to subtract the contribution due to the decay $\Sigma^0 \to \gamma\Lambda$, since the photon was typically not measured[1]. For this reason, the inclusive $\Lambda/\overline{\Lambda}$ yield here considered is both due to the production in prompt reactions, as well as due to the decay of short-lived hyperons. When performing Monte Carlo simulations, all $\Lambda/\overline{\Lambda}$ in the final state were thus taken into account, independently from their origin.

**20 GeV photon beam** The data employed for the comparison was measured by the SLAC Hybrid Facility Photon Collaboration [11, 12] using the SLAC 1-m hydrogen-bubble-chamber detector [22] exposed to the photon beam produced via the back-scattering of a frequency-quadrupled $7.11{\cdot}10^{15}$ Hz Nd:YAG laser beam with a 30-GeV electron beam, resulting in an almost-monochromatic 20 GeV spectrum, with a full width at half of about 2 GeV [23].

The collaboration measured the inclusive production of $\Lambda$ and $\bar{\Lambda}$ hyperons, $\gamma p \to \Lambda/\bar{\Lambda}X$, reporting the total cross sections and the invariant distribution of the Feynmann-$x$ variable, defined as:

$$x = 2p_L^{CM}/\sqrt{s} \tag{6}$$

where $p_L^{CM}$ is the $\Lambda/\bar{\Lambda}$ longitudinal momentum in the $\gamma - p$ reference frame and $s$ is the initial state invariant mass squared - for a 20 GeV photon beam, $s \simeq 38$ GeV$^2$. The Feynmann-$x$ invariant

[1]For the experiment described in [11] the inclusive $\Sigma_0$ photoproduction cross section was measured by identifying the final state photon via its conversion to an $e^+e^-$ pair within the target.

| Reaction | Data | FLUKA | GEANT4 |
|---|---|---|---|
| $\gamma p \to \Lambda X$ | $5.6 \pm 0.2$ $\mu$barn | 5.6 $\mu$barn | 6.17 $\mu$barn |
| $\gamma p \to \bar{\Lambda} X$ | $0.39 \pm 0.04$ $\mu$barn | 0.4 $\mu$barn | 1.75 $\mu$barn |

Table 2: Inclusive $\Lambda$ and $\bar{\Lambda}$ photoproduction cross sections for a 20 GeV impinging photon beam.

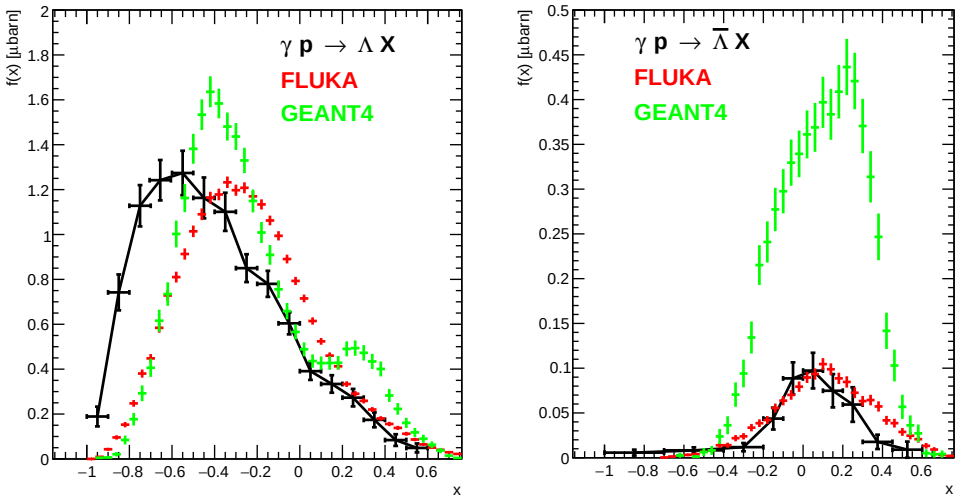


Figure 2: Distribution of $f(x) \equiv F(x)$ for inclusive $\Lambda$ (left) and $\overline{\Lambda}$ photoproduction on the proton, for 20 GeV beam energy, comparing experimental results from Ref. [12] with the predictions from FLUKA (red) and GEANT4 (green).

distribution $F(x)$ reads:

$$F(x) = \frac{1}{\sigma_{TOT}} \frac{2E(x)}{\pi\sqrt{s}} \frac{d\sigma}{dx} \tag{7}$$

where $E(x)$ is the average $\Lambda/\bar{\Lambda}$ energy in the $\gamma - p$ reference frame for a fixed $x$ value, and $\sigma_{TOT}$ is the total $\gamma - p$ interaction cross section. For the latter, the collaboration assumed a value $\sigma_{TOT} = 115 \pm 2$ $\mu$barn. In order to make a data-MC comparison focused only on this reaction, and not depending on the total $\sigma - p$ interaction cross-section, we considered the product $f(x) \equiv F(X) \cdot \sigma_{TOT}$.

The total cross sections for the $\Lambda$ and for the $\bar{\Lambda}$ inclusive photoproduction reactions are reported in Tab. 2. FLUKA perfectly reproduces the experimental data for both reactions. On the contrary, GEANT4 results slightly overestimate the $\Lambda$ production, and are a factor $4.5$ higher for the $\bar{\Lambda}$ production.

The distribution of $f(x)$ is reported in Fig. 2 for both reactions, comparing data (black points) with MC predictions from FLUKA (red points) and GEANT4 (green points). For $\Lambda$ production, both Monte Carlo codes are generally in good agreement with data, but predict an invariant Feynman-$x$ distribution shifted at slightly higher values of $x$. The GEANT4 result also features a peak at $x \simeq 0.3$ not seen in the data. For $\bar{\Lambda}$ production, instead, while the FLUKA result is in very good agreement with data, both in terms of the shape and of the normalization of $f(x)$, GEANT4 result, while reproducing the shape of $f(x)$, predicts a normalization that is

approximately 4.5 larger than the one seen in the data.

**25-75 GeV photon beam** The data employed for the comparison was measured by the Bonn-CERN-École Poly.-Glasgow-Lancaster-Manchester-Orsay-Paris(VI)-Paris(VII)-Rutherford-Sheffield Collaboration using the OMEGA spectrometer and a tagged photon beam at CERN SPS (WA4 experiment) [22]. The collaboration measured the differential cross section $\frac{d\sigma}{dx}$ for inclusive $\Lambda$ and $\overline{\Lambda}$ photoproduction on the proton for 5 photon beam energy intervals. The experimental results are reported in Fig. 3 and Fig. 4, together with the predictions from FLUKA and GEANT4. For $\Lambda$ production, the measured cross section is almost constant with respect to the beam energy, and decreases rapidly with increasing $x$. These main features are well reproduced by both Monte Carlo codes, although the GEANT4 prediction features a secondary peak in the $d\sigma/dx$ shape at $x \simeq 0.3$, in particular at lower beam energies, not justified by data. Both codes qualitatively reproduce the overall cross-section normalization - FLUKA always predicts smaller values, while in GEANT4, due to the more sizable energy dependence of this observable, the prediction under (over) estimates the data at lower (higher) beam energy. For $\overline{\Lambda}$ production, instead, while still the experimental results are almost independent of the beam energy, the shape of $d\sigma/dx$ is more symmetric around $x = 0$ - both Monte Carlo codes reproduce qualitatively this feature, but predict a significant dependency on the beam energy. Concerning the overall normalization, FLUKA is generally in better agreement with the data, while GEANT4 over-estimates the cross section by a factor up to $\simeq 3$ for the highest photon beam energy interval.

### *3.2 Case-2: exclusive $\pi^+$ protoproduction at backward and forward angles*

The reaction $\gamma p \to \pi^+ n$ can be a significant source of background events in POKER, in particular, if the charged pion is produced at backward angles ($u \simeq 0$), out of the detector acceptance, with only the neutron going in the forward direction, this particle being more challenging to detect in the HCAL.

The data employed for the comparison was measured at SLAC [14] by Anderson *et al.*, who reported the value of the differential cross section $d\sigma/du$ for photon beam energies between 5 GeV and 15.5 GeV and $u$ values between -0.7 GeV$^2$ and +0.05 GeV$^2$. The experimental results are reported in Fig. 5, left panel, together with the predictions from FLUKA and GEANT4[2].

In order to "isolate" this reaction from the Monte Carlo results (both for FLUKA and for GEANT4), we filtered the Monte Carlo events keeping those with exactly one $\pi^+$ and one $n$ emerging from the target, and then we computed the corresponding missing energy $M_E$, selecting events with $M_E \simeq 0$. This guarantees the exclusivity of the final state. It should be noted that, during preliminary tests with GEANT4, we observed that no events at all corresponding to this reaction were produced. We explained this from the fact that, in the default GEANT4 configuration, photonuclear reactions for photon beam energies in the range here considered are modeled through the

[2]Unfortunately, no numerical data for $d\sigma/du$ are reported in Ref. [14], and the quality of the plot showing $k^3 d\sigma/du$ as a function of $u$, $k$ being the photon energy in the laboratory frame, does not allow to disentangle data points corresponding to different beam energies. Therefore, for simplicity we assumed a "universal" shape for the measured $k^3 d\sigma/du$ observable, independent from the photon energy.

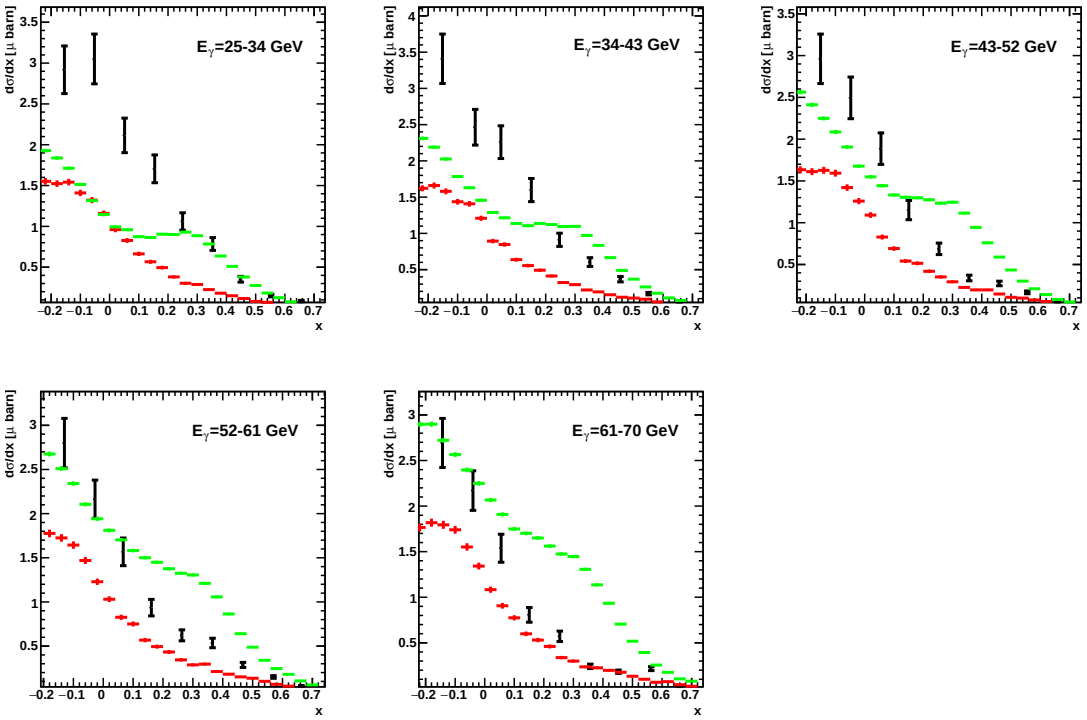


Figure 3: Differential cross section $d\sigma/dx$ for inclusive $\Lambda$ photoproduction, for five photon beam energy bins. The black points are the experimental results reported in Ref. [13], while the red and green points are the predictions from FLUKA and GEANT4 respectively.

Fritiof string model, that, probably, while being able to reproduce the inclusive yield of final-state particles in photo-induced nuclear processes, is not capable of handling individually the different photo-nuclear reaction channels. Therefore, we modified the energy point at which the Bertini cascade model fades out in favor of the string model, setting it to 25 GeV. By doing so, we were able to observe events corresponding to the $\pi^+ - n$ photoproduction reaction.

From this study, we concluded that the FLUKA results reproduce quite well the experimental data, which is characterized by a peak at $u \simeq 0$, which is associated with a sub-dominant $u$-channel pole contribution in the reaction amplitude. The GEANT4 result, instead, does not reproduce this feature, and predicts an almost null cross-section for $u \simeq 0$. This conclusion is in agreement with that obtained from the LDMX collaboration, which performed a detailed study of the implementation of this reaction in GEANT4 [24]. In particular, they found that the description of the $u$-channel pole is absent for energies above few GeV, where the description of this process based on a data-driven model is abandoned in favor of a parameterization that only includes the $t-$channel singularity.

The differential cross section $\frac{d\sigma}{dt}$ for $k = 5$ GeV measured by Boyarski and collaborators [15] is reported in Fig. 5, right panel, comparing again the results from FLUKA and GEANT4. For the latter, we again employed the modification for the Bertini-to-string model energy transition point described before. Interestingly, at low-$t$ both Monte Carlo codes predict a similar cross-section shape, however, the overall normalization is approximately one order of magnitude

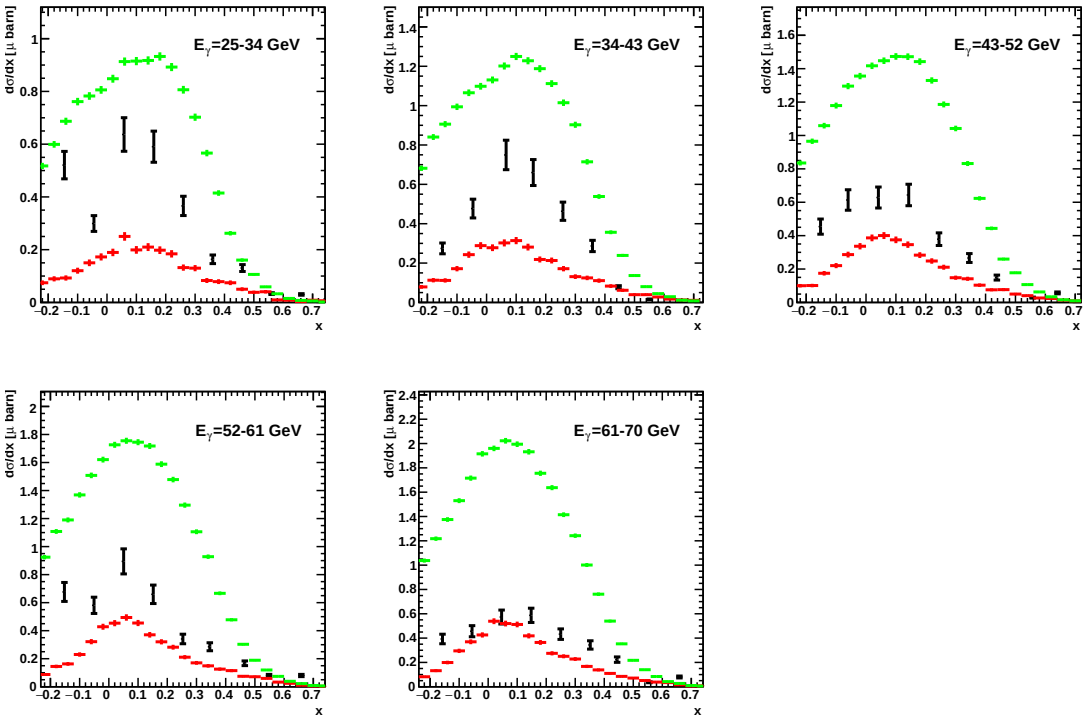


Figure 4: Same as Fig. 3, for inclusive $\overline{\Lambda}$ production.

smaller than the measured one.

## 4 Conclusions

In this work, we investigated the implementation of a few photo-nuclear reactions in the GEANT4 and FLUKA Monte Carlo programs, comparing the results obtained from these codes with the real data available in the literature. Specifically, we focused on the inclusive $\Lambda$ and $\bar{\Lambda}$ photoproduction on the proton at $E_\gamma \gtrsim 10$ GeV, and on the exclusive $\pi^+$ photoproduction at backward angles, comparing the differential cross sections. We found that both Monte Carlo codes reproduce the correct order of magnitude for the cross-section of these processes, with non-negligible differences in the corresponding shape. In general, the results from FLUKA are closer to the real data than those from GEANT4.


### Acknowledgments

This result is part of a project that has received funding from the European Research Council (ERC) under the European Union's Horizon 2020 research and innovation program, Grant agreement No. 947715 (POKER).

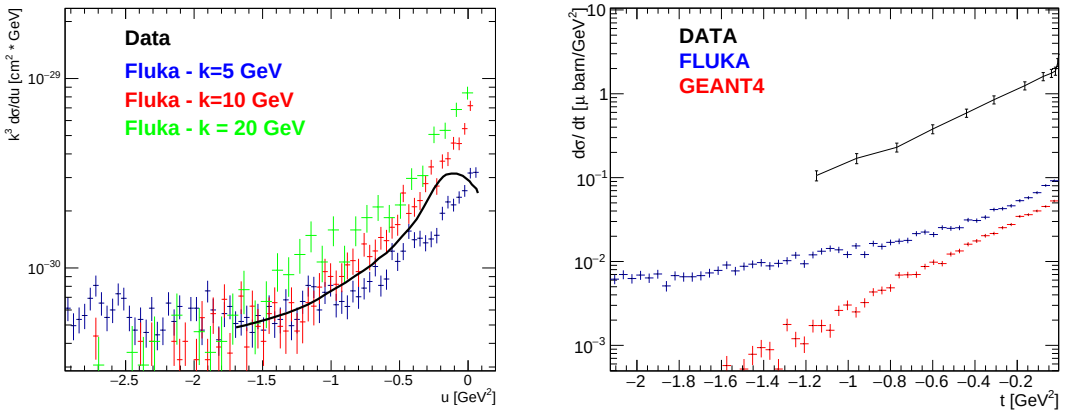


Figure 5: Left: differential cross section $k^3 d\sigma/du$ for the exclusive $\gamma p \to \pi^+ n$ reaction, with $k$ being the photon energy in the laboratory frame. The black line is the experimental result from Ref. [14], while the blue, red, and green points are the results obtained from the FLUKA simulation. Right: differential cross section $d\sigma/dt$ for the exclusive $\gamma p \to \pi^+ n$ reaction, for $k = 5$ GeV. The black line is the experimental result from Ref. [15], while the blue and red points are the results obtained from FLUKA and GEANT4, respectively.

## References


[1] L. Roszkowski, E. M. Sessolo, and S. Trojanowski. "WIMP dark matter candidates and searches—current status and future prospects". In: *Rept. Prog. Phys.* 81.6 (2018), p. 066201. arXiv: 1707.06277 [hep-ph].

[2] G. Arcadi et al. "The waning of the WIMP? A review of models, searches, and constraints". In: *Eur. Phys. J. C* 78.3 (2018), p. 203. arXiv: 1703.07364 [hep-ph].

[3] B. Holdom. "Two U(1)'s and Epsilon Charge Shifts". In: *Phys. Lett. B* 166 (1986), pp. 196–198.

[4] A. R. Liddle. *An introduction to modern cosmology*. Ed. by Wiley. 2003.

[5] L. Marsicano et al. "Novel Way to Search for Light Dark Matter in Lepton Beam-Dump Experiments". In: *Phys. Rev. Lett.* 121.4 (2018), p. 041802. arXiv: 1807.05884 [hep-ex].

[6] D. Banerjee et al. "Dark matter search in missing energy events with NA64". In: *Phys. Rev. Lett.* 123.12 (2019), p. 121801. arXiv: 1906.00176 [hep-ex].

[7] A. Chilton. "A note on the fluence concept". In: *Health Physics* 34.6 (1978), pp. 715–716.

[8] K. Schilling and G. Wolf. "How to analyze vector meson production in inelastic lepton scattering". In: *Nucl. Phys. B* 61 (1973), pp. 381–413.

[9] S. J. Brodsky and J. Pumplin. "Photon-Nucleus Total Cross-Sections". In: *Phys. Rev.* 182 (1969), pp. 1794–1804.

[10] J. Ranft and W. R. Nelson. "Hadron cascades induced by electron and phtons beams in the GeV energy range". In: *Nucl. Instrum. Meth. A* 257 (1987), p. 177.

[11] K. Abe et al. "Inclusive Photoproduction of Strange Baryons at 20-GeV". In: *Phys. Rev. D* 32 (1985), pp. 2869–2882.

[12] K. Abe et al. "Inclusive Photoproduction of Neutral Strange Particles at 20-GeV". In: *Phys. Rev. D* 29 (1984), p. 1877.

[13] D. Aston et al. “Inclusive Production of Lambdas and Anti-lambdas in $\gamma p$ Interactions for Photon Energies Between 25-GeV and 70-GeV”. In: *Nucl. Phys. B* 195 (1982), pp. 189–202.

[14] R. L. Anderson et al. “HIGH-ENERGY PHOTOPRODUCTION OF CHARGED PIONS AT BACKWARD ANGLES”. In: *Phys. Rev. Lett.* 23 (1969), pp. 721–724.

[15] A. Boyarski et al. “5-GeV - 16-GeV SINGLE pi+ PHOTOPRODUCTION FROM HYDROGEN”. In: *Phys. Rev. Lett.* 20 (1968), pp. 300–303.

[16] G. Battistoni et al. “Hadron production simulation by FLUKA”. In: *J. Phys. Conf. Ser.* 408 (2013). Ed. by A. Blondel, I. Efthymiopoulos, and G. Prior, p. 012051.

[17] A. Capella et al. “Dual parton model”. In: *Phys. Rept.* 236 (1994), pp. 225–329.

[18] J. P. Wellisch, M. Kossov, and P. Degtyarenko. “Electro and gamma nuclear physics in GEANT4”. In: *eConf* C0303241 (2003), THMT004. arXiv: `nucl-th/0306012`.

[19] G. Folger and J. P. Wellisch. “String parton models in GEANT4”. In: *eConf* C0303241 (2003), MOMT007. arXiv: `nucl-th/0306007`.

[20] D. H. Wright and M. H. Kelsey. “The Geant4 Bertini Cascade”. In: *Nucl. Instrum. Meth. A* 804 (2015), pp. 175–188.

[21] M. Ungaro et al. “The CLAS12 Geant4 simulation”. In: *Nucl. Instrum. Meth. A* 959 (2020), p. 163422.

[22] D. Aston et al. “Jet Like Structure in the Reaction $\gamma p \to \pi^+\pi^-\pi^+\pi^-\pi^+\pi^- p$”. In: *Nucl. Phys. B* 166 (1980), pp. 1–24.

[23] J. E. Brau et al. “The Lead Glass Columns: A Large Shower Detector at the SLAC Hybrid Facility”. In: *Nucl. Instrum. Meth.* 196 (1982), p. 403.

[24] T. Åkesson et al. “Light Dark Matter eXperiment (LDMX)”. In: (Aug. 2018). arXiv: `1808.05219 [hep-ex]`.